Model Order Reduction for Managed Pressure Drilling Systems based on a model with local nonlinearities

Lordejani, S. Naderi; Besselink, B.; Abbasi, M. H.; Kaasa, G. O.; Schilders, W. H.A.; van de Wouw, N.

DOI
10.1016/j.ifacol.2018.06.354

Publication date
2018

Document Version
Final published version

Published in
IFAC-PapersOnLine

Available online at www.sciencedirect.com

ScienceDirect

IFAC Papers Online CONFERENCE PAPER ARCHIVE

IFAC PapersOnLine 51-8 (2018) 50–55

Model Order Reduction for Managed Pressure Drilling Systems based on a Model with Local Nonlinearities ⋆

S. Naderi Lordejani * **B. Besselink** ** **M. H. Abbasi** *** **G.-O. Kaasa** **** **W. H. A. Schilders** *** **N. van de Wouw** *,†,‡

* *Department of Mechanical Engineering, Eindhoven University of Technology, Eindhoven, The Netherlands (s.naderilordejani@tue.nl, n.v.d.wouw@tue.nl)*

** *Johann Bernoulli Institute for Mathematics and Computer Science, University of Groningen, Groningen, The Netherlands (b.besselink@rug.nl)*

*** *Department of Mathematics and Computer Science, Eindhoven University of Technology, The Netherlands (m.h.abbasi@tue.nl, w.h.a.schilders@tue.nl)*

**** *Kelda Drilling Controls, Porsgrunn, Norway (gok@kelda.no)*

† *Department of Civil, Environmental & Geo-Engineering, University of Minnesota, Minneapolis, USA*

‡ *Delft Center for Systems and Control, Delft University of Technology, Delft, The Netherlands*

Abstract: Automated Managed Pressure Drilling (MPD) is a method for fast and accurate pressure control in drilling operations. The achievable performance of automated MPD is limited, firstly, by the control system and, secondly, by the hydraulics model based on which this control system is designed. Hence, an accurate hydraulics model is needed that, at the same time, is simple enough to allow for the use of high performance controller design methods. This paper presents an approach for nonlinear Model Order Reduction (MOR) for MPD systems. For a single-phase flow MPD system, a nonlinear model is derived that can be decomposed into a feedback interconnection of a high-order linear subsystem and low-order nonlinear subsystem. This structure, under certain conditions, allows for a nonlinear MOR procedure that preserves key system properties such as stability and provides a computable error bound. The effectiveness of this MOR method for MPD systems is illustrated through simulations.

Keywords: Managed Pressure Drilling, Model Order Reduction, Automatic Control, Modeling.

1. INTRODUCTION

Drilling for oil and gas is performed in the presence of a circulating drilling fluid called drilling mud. The mud is pumped into the drillstring at high pressure. At the well bottom, it leaves the drillstring through nozzles at the bit to enter the annulus. It then flows up through the annulus, carrying rock cuttings out of the well. Moreover, the mud is used to control the annulus pressure within a specific range to avoid, on the one hand, an influx from surrounding formations and, on the other hand, fracturing the formations. This is conventionally accomplished by changing the mud density. However, this method is slow and inaccurate and it lacks a means of compensating transient pressure fluctuations.

To overcome such drawbacks of conventional pressure control methods, the method of managed pressure drilling (MPD) has been introduced, see e.g. Stamnes et al. (2008). In MPD, the annulus is sealed off at the top with a rotating control device and the mud is circulated out of the well through a choke valve, see Fig. 1. This combination provides a surface back pressure that can be controlled by changing the choke opening. In automated MPD systems, the surface pressure, and thereby the Bottom-Hole Pressure (BHP), is controlled by an automatic control system Mahdianfar and Pavlov (2017); Kaasa et al. (2012).

The performance of the control system of an automated MPD system is dependent not only on the controller design, but also on the hydraulics model used for designing the control system. This model should be accurate enough to capture the essential hydraulic characteristics and, at the same time, the complexity of the model should be restricted to facilitate the application of established system-theoretic analysis and design techniques. Existing low-complexity models, such as in Kaasa et al. (2012), are, however, incapable of capturing essential transients such as the propagation of pressure waves. Ignoring such phenomena in modeling and controller design can cause a failure in the accomplishment of control objectives. It can even cause instability, which is especially probable in the case of long wells Landet et al. (2013). The goal of this paper is to construct a high-fidelity, though low-complexity, model for single-phase flow MPD systems for control purposes.

For many drilling scenarios, an MPD system can be described accurately by a system of linear hyperbolic

⋆ This research has been carried out in the HYDRA project, which has received funding from the European Union's Horizon 2020 research and innovation program under grant agreement No 675731.

10.1016/j.ifacol.2018.06.354

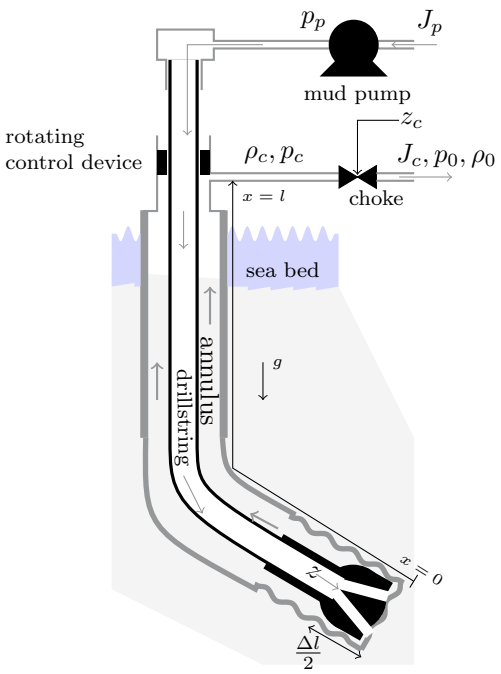

Fig. 1. A simplified schematic diagram of an MPD system.

Partial Differential Equations (PDEs) (see Aarsnes et al. (2012)) and accompanying boundary equations. These boundary conditions are implicit and highly nonlinear, but act only locally. For controller design, we are more interested in system descriptions in the form of low-order models in terms of Ordinary Differential Equations (ODEs), for which control theory is well developed. This ODE model can be obtained by spatially discretizing the PDE, but the resulting discretized model is typically of high order and hence not suitable for controller synthesis.

Model reduction may at this point be employed to obtain a low-order approximation inheriting the key properties of the original model. Model reduction for MPD applications has been investigated, but to a limited extent. Mahdianfar et al. (2012) used a linear MOR method for controller reduction. Using a staggered-grid approach, Landet et al. (2012) derived a high-order model and used a linear model reduction method for reducing that model. In a later work, Landet et al. (2013) reduced the complexity of their model simply by using a low resolution coarse discretization of the PDE model. This however lacks a quantitative measure on the achieved accuracy. Nonlinear MOR in the context of MPD automation is therefore still an open issue which deserves more attention. In this paper, given 1) the spatially discretized ODE model combined with 2) (local) nonlinear boundary conditions, the resulting model is a nonlinear system comprising high-order linear dynamics with local nonlinearities. For this class of systems, a MOR procedure has been recently developed by Besselink et al. (2013). This method, unlike many other MOR methods for nonlinear systems, preserves key system properties (such as $\mathcal{L}_2$ stability). Moreover, it provides a computable error bound on the error induced by the reduction.

The main contributions of this paper are twofold. First, a control-relevant hydraulics model is developed for single-phase flow MPD systems. The model is obtained by employing a high-resolution discretization scheme for the PDE equations and a characteristics-based method for dealing with the nonlinear boundary conditions. Second, in view of its particular structure, the complexity of the resulting nonlinear model is reduced by employing the above-mentioned MOR method.

The rest of this paper is organized as follows. Section 2 is devoted to the mathematical modeling of the system. In Section 3, the MOR procedure is described. Illustrative simulation results are presented in Section 4 and, finally, conclusions are presented in Section 5.

2. MATHEMATICAL MODELING

An MPD system can be regarded as two long pipes which are connected through a bit in the middle. Moreover, the inlet and outlet of the connected pipes are connected to the pump and choke, respectively. In what follows, a model is derived for the system based on this description and the schematic diagram in Fig. 1.

2.1 Flow model in a single pipe

PDE model: A single-phase laminar flow, which is the case in many drilling scenarios, in a pipe can accurately be described by the linear PDE system (see Aarsnes et al. (2012))

$$\frac{\partial q}{\partial t} + \Psi \frac{\partial q}{\partial x} = F(x)q, \tag{1}$$

with

$$q = \begin{bmatrix} \rho \\ \rho v \end{bmatrix}, \Psi = \begin{bmatrix} 0 & 1 \\ c_l^2 & 0 \end{bmatrix}, F = \begin{bmatrix} 0 & 0 \\ g\sin(\theta(x)) & -\dfrac{32\mu_m}{\rho_0 d^2} \end{bmatrix},$$

and where $x \in [0, l]$ and t are the spatial and time variables, respectively, and l is the length of the pipe. The liquid density, velocity, and pressure are denoted by $\rho(x,t)$, $v(x,t)$ and $p(x,t)$, respectively, whereas μ_m, d, $\theta(x)$, g and c_l are the liquid viscosity, the hydraulic diameter of the pipe, the pipe inclination, gravitational acceleration, and sound velocity in liquid, respectively. Note that a linear PDE model is used to avoid distributed nonlinearities in the ODE model to be derived. The equation of state, describing the relation between the pressure and density, is chosen as in Kaasa et al. (2012), i.e.,

$$p = c_l^2 (\rho - \rho_0) + p_0, \tag{2}$$

where p_0 and ρ_0 are the reference pressure and density, respectively. The inlet and outlet boundary conditions are implicitly given as

$$f_1(q(0,t)) = 0, \quad f_2(q(l,t)) = 0, \tag{3}$$

where $f_1(\cdot)$ and $f_2(\cdot)$ are given boundary functions.

Model discretization: By applying a first-order Kurganov-Tadmor (KT) scheme (see Kurganov and Tadmor (2000)) to discretize the PDE (1), one obtains

$$\dot{Q}^i(t) = A_1 Q^{i-1}(t) - A_2^i Q^i(t) + A_3 Q^{i+1}(t), i = \{1, ..., n\}, \tag{4}$$

where the spatial domain is discretized into n cells $G_i = \left(x_{i-\frac{1}{2}}, x_{i+\frac{1}{2}}\right)$ of length Δx, with $x_{i+\frac{1}{2}} = i\Delta x$ called the i^{th} cell interface and $x_i = (i - \frac{1}{2})\Delta x$ marking the middle point of this cell. The variable $Q^i(t)$ is an approximate of the spatial average of the vector $q(x,t)$ over G_i. Also,

$A_1 = \frac{c_l}{2\Delta x} I_2 + \frac{1}{2\Delta x}\Psi$, $A_2^i = F(x_i) + \frac{c_l}{\Delta x} I_2$, $A_3 = \frac{c_l}{2\Delta x} I_2 - \frac{1}{2\Delta x}\Psi$, with I_m the $(m \times m)$ identity matrix.

Boundary condition treatment: Expanding (4) for $i = 1$ and $i = n$, one encounters dependencies on Q^0 and Q^{n+1}. These variables are used as approximates of the boundary conditions $q(t, 0)$ and $q(t, l)$, respectively. Taking a characteristics-based approach similar to the one in Fjelde and Karlsen (2002), one finally arrives at

$$\begin{aligned} Q^0(t) =& a_w W^0(t) + b\frac{J_{in}(t, Q_1^0)}{2\phi^p}, \\ Q^{n+1}(t) =& - a_w W^{n+1}(t) - b\frac{J_{out}(t, Q_1^{n+1})}{2\phi^p}, \end{aligned} \tag{5}$$

where $W^0(t)$ and $W^{n+1}(t)$ are the solutions of

$$\begin{aligned} \dot{W}^0 =& -\lambda W^0 - (L_2 F(x_1) - \lambda L_2)\, Q^1, \\ \dot{W}^{n+1} =& -\lambda W^{n+1} - (L_1 F(x_n) - \lambda L_1)\, Q^n, \end{aligned} \tag{6}$$

and J_{in} and J_{out} are the the inlet and outlet mass flow rates, respectively. These are determined from the boundary conditions (3). Also, ϕ^p is the pipe cross sectional area, $\lambda = \frac{c_l}{\Delta x}$, $L_1 = 0.5\,[\, c_l \;\; 1\,]$, $L_2 = 0.5\,[\, -c_l \;\; 1\,]$, $a_w = [\, 2/c_l \;\; 0\,]^T$ and $b = [\, 0 \;\; 1\,]^T$.

Finally, by combining (4)-(6), one can write the hydraulics model in a pipe in a state-space form as

$$\begin{cases} \dot{Q}_p =& A^p Q_p + B_u^p u^p + B_w^p w^p, \\ v^p =& C_v^p Q_p + D_{vu}^p u^p + D_{vw}^p w^p, \end{cases} \tag{7}$$

where the superscript (sometimes subscript) p refers to the pipe, $Q_p = \left[\, W^0 \;\; \left(Q^1\right)^T \;\; \ldots \;\; \left(Q^n\right)^T \;\; W^{n+1} \,\right]^T \in \mathbb{R}^{2n+2}$ is the state vector and

$$\begin{aligned} u^p =& \frac{J_{in}(t, v_1^p)}{2\phi^p} \in \mathbb{R}, \quad w^p = \frac{J_{out}(t, v_2^p)}{2\phi^p} \in \mathbb{R}, \\ v^p =& [v_1^p, v_2^p]^T = [Q_1^0, Q_1^{n+1}]^T \in \mathbb{R}^2. \end{aligned} \tag{8}$$

The variable u^p, imposed by $f_1(\cdot)$ in (3), is the mass flow rate (with a constant factor) at the inlet and it may be assumed as an input to the system. Next, w^p is a feedback signal from the nonlinear term due to $f_2(\cdot)$. The vector v^p, consisting of the densities at the inlet and outlet, provides the inputs to the nonlinear term.

2.2 MPD modeling

The MPD system can be modeled by a series connection of two pipe models of the form (7). The hydraulic dynamics in the drillstring and in the annulus are both described by (7), by changing sub/superscript p by d and a, respectively. Next, we specify the system boundary conditions.

Boundary conditions: The first boundary equation imposed by the pump equation is given as

$$J_p(t) - \phi^d q_2^d(0, t) = 0, \tag{9}$$

where J_p is the pump mass flow rate. The second and the third boundary equations describe the outlet of the drillstring and the inlet of the annulus. Those are derived using the bit equation and are as follows:

$$z(t) - \phi^d q_2^d(l, t) = 0, \quad z(t) - \phi^a q_2^a(0, t) = 0, \tag{10}$$

where $z(t)$ represents the mass flow rate through the bit which is given by the nonlinear bit model

$$\dot{z} = \begin{cases} -\beta_1 z^2 - \beta_2 z + \beta_3 \Delta\rho_{dh}, \text{for} & z > 0, \\ \max(0, -\beta_1 z^2 - \beta_2 z + \beta_3 \Delta\rho_{dh}), \text{for} & z = 0, \end{cases} \tag{11}$$

where $\Delta\rho_{dh} = q_1^d(l, t) - q_1^a(0, t)$, and the parameters β_1, β_2 and β_3 are dependent on the well parameters and the bit parameters C_d and A_n, which are the bit constant and the equivalent bit nozzle area, respectively. To derive this bit model, a control volume of a length of Δl is taken over the bit and an approach similar to the one in Kaasa et al. (2012) is followed. The $\max(\cdot)$ operator is used to model a non-return value installed above the bit in the drillstring. The reason for using this dynamical equation rather than a static bit equation is to prevent a chattering in the inlet boundary variables when the flow is close to zero.

The last boundary equation is given by the choke equation

$$J_c(q_2^a(l, t)) - k_c c_l G(z_c) f_c\left(q_1^a(l, t)\right) = 0, \tag{12}$$

where J_c, k_c, $z_c(t)$ and $G(z_c)$ are the choke mass flow rate, the choke flow factor, the choke opening and the choke characteristic, respectively. Also, $f_c(q_1^a(l, t)) = sgn(r)\sqrt{|r|}$, where $r = 2q_1^a(l, t)(q_1^a(l, t) - \rho_0)$.

Finite-dimensional model: Note that if the drillstring inclination is $\theta(x)$, then that of the annulus is $-\theta(l - x)$. With this in mind and based on the explanation in the beginning of Section 2.2, one may derive the model for an MPD system to obtain a representation of the form

$$\Sigma_{lin} : \begin{cases} \dot{X} = AX + B_u u_1 + B_w W, \\ V = C_v X + D_{vu} u_1 + D_{vw} W, \end{cases} \tag{13}$$

$$\Sigma_{nl} : \begin{cases} \dot{z} = \begin{cases} -\beta_1 z^2 - \beta_2 z + \beta_3 \Gamma V, \text{for} & z > 0, \\ \max(0, -\beta_1 z^2 - \beta_2 z + \beta_3 \Gamma V), \text{for} & z = 0, \end{cases} \\ W = Cz + h(V, u_2), \end{cases} \tag{14}$$

where $X = \left[\, Q_d^T \;\; Q_a^T \,\right]^T \in \mathbb{R}^{2n+4}$, and z are the state variables. Note that the number of cells (as used in discretization) for the drillstring and for the annulus are the same and equal to n. The vector $V = [\, V_1 \;\; V_2 \;\; V_3 \,]^T = [\Gamma_2 v^d, (v^a)^T]^T \in \mathbb{R}^3$, with $\Gamma_2 = [\, 0 \;\; 1 \,]$, contains the fluid densities at the well bottom and choke, and $W = \left[\, w^d \;\; u^a \;\; w^a \,\right]^T$. The exogenous inputs to the system are

$$u_1 = u^d = \frac{J_p}{2\phi^d}, \quad u_2 = \frac{k_c c_l G(z_c)}{2\phi^a}, \tag{15}$$

and also

$$h(V, u_2) = [\, 0 \;\; 0 \;\; u_2 f_c(V_3) \,]^T. \tag{16}$$

In output-feedback control problems, the outputs of the system, the BHP in this case, are to be available for measurement. However, the measurements of the BHP are communicated at a low rate, are usually delayed and unreliable. Thus, we choose the choke density ρ_c (convertible to pressure using (2)) as the output here, which is to be well approximated by the reduced-order model in Section 3. The BHP measurements can then be used to update an estimator generating the setpoint for the choke pressure. The choke density is denoted by V_3, thus

$$y = V_3 = \Gamma_y V, \quad \Gamma_y = [\, 0_{1\times 2} \;\; 1 \,]^T, \tag{17}$$

where $y \in \mathbb{R}$ is the output.

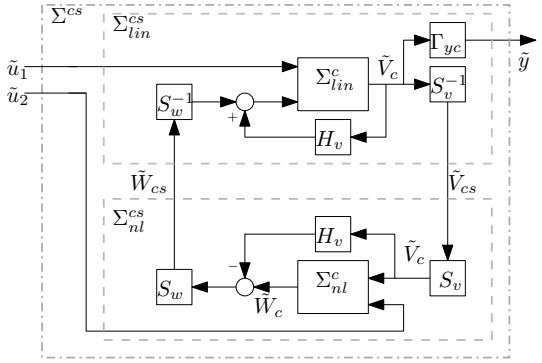

Fig. 2. A block diagram of the system in the presence of the loop transformations.

2.3 Model reformulation

To facilitate later analysis, we will first transform the model into a suitable form by performing two loop transformations. In addition, assuming that $z(t) > 0$, the linear part of the nonlinear dynamics (14) is merged into the linear subsystem (13), allowing for rewriting the system in a Lur'e-type form, composed of an interconnection of a linear subsystem and a nonlinear static mapping. Moreover, most of the drilling time is spent on the drilling ahead operation, during which the pump flow rate is kept constant at some nominal value J_p^* and the choke opening only has small variations around a nominal value z_c^*, to compensate for transient pressure fluctuations. Thus, it is reasonable to change the origin of the resulting Lur'e-type system to an operating point $X_c^* = [X^{*T}, z^*]^T$ and denote the transformed system by $\Sigma^c = (\Sigma^c_{lin}, \Sigma^c_{nl})$, with Σ^c_{lin} and Σ^c_{nl} the linear subsystem and nonlinear mapping, respectively. Note that X_c^* corresponds to the inputs $u_1^* = \frac{J_p^*}{2\phi^d}$ and $u_2^* = \frac{k_c c_l G(z_c^*)}{2\phi^a}$. The value z_c^* is designed such that the resulting surface pressure is larger than the reference pressure p_0 for normal drilling operations to avoid a saturation in the choke opening. After performing the loop transformations as illustrated in the block diagram in Fig. 2 and a change of coordinates, as introduced above, we obtain the Lur'e-type system

$$\Sigma^{cs}_{lin}: \begin{cases} \dot{\tilde{X}}_c = A_c\tilde{X}_c + B_{uc}\tilde{u}_1 + B_{ws}\tilde{W}_{cs}, \\ \tilde{V}_{cs} = C_{vs}\tilde{X}_c + D_{vsu}\tilde{u}_1 + D_{vsw}\tilde{W}_{cs}, \\ \tilde{y} = \Gamma_{ys}\tilde{V}_{cs}, \end{cases} \tag{18}$$

$$\Sigma^{cs}_{nl}: \tilde{W}_{cs} = S_w\tilde{h}_c(S_v\tilde{V}_{cs}, \tilde{u}_2), \tag{19}$$

where $X_c = \begin{bmatrix} X^T & z \end{bmatrix}^T \in \mathbb{R}^{n_c}$ with $n_c = 4n + 5$, and $V_c = \begin{bmatrix} V_{c1} & V_{c2} \end{bmatrix}^T = \begin{bmatrix} z & V_3 \end{bmatrix}^T \in \mathbb{R}^2$, $V_{cs} = S_v^{-1}V_c$, $W_{cs} = S_wW_c$. A tilde "˜" indicates the difference between a variable and its operational value denoted by *, and

$$h_c(V_c, u_2) = \bar{h}(V_c, u_2) - H_vV_c, \tag{20}$$

where $\bar{h} = \begin{bmatrix} V_{c1}^2 & u_2 f_c(V_{c2}) \end{bmatrix}^T$. Finally, $H_v = diag(\alpha_b, \alpha_c)$, S_v and S_w are related to the loop transformations seen in Fig. 2 and are yet to be determined.

3. NONLINEAR MODEL ORDER REDUCTION

3.1 Model order reduction procedure

The nonlinear model (18) and (19), denoted by $\Sigma^{cs} = (\Sigma^{cs}_{lin}, \Sigma^{cs}_{nl})$, is in the form of a feedback interconnection of a high-order linear subsystem Σ^{cs}_{lin} and low-order nonlinear subsystem Σ^{cs}_{nl}. This particular structure enables us to reduce the model complexity by only reducing the linear subsystem using existing MOR techniques for linear systems, such as balanced singular perturbation (see Fernando and Nicholson (1982); Liu and Anderson (1989)), which preserves the steady-state response. This leads to a reduced-order linear subsystem $\hat{\Sigma}^{cs}_{lin}$ of the following form

$$\hat{\Sigma}^{cs}_{lin}: \begin{cases} \dot{\hat{\tilde{X}}}_c = \hat{A}_c\hat{\tilde{X}}_c + \hat{B}_{uc}\tilde{u}_1 + \hat{B}_{ws}\hat{\tilde{W}}_{cs}, \\ \hat{\tilde{V}}_{cs} = \hat{C}_{vs}\hat{\tilde{X}}_c + \hat{D}_{vsu}\tilde{u}_1 + \hat{D}_{vsw}\hat{\tilde{W}}_{cs}, \\ \hat{\tilde{y}} = \Gamma_{ys}\hat{\tilde{V}}_{cs}, \end{cases} \tag{21}$$

where $\hat{\tilde{X}}_c \in \mathbb{R}^k$, $k < n_c$, and the dimensions of the inputs and outputs remain unchanged. Balancing-based MOR methods preserve stability and minimality, and provide a bound on the reduction error of the linear subsystem, such that for the H_∞-norm of the difference between Σ^{cs}_{lin} (with $\tilde{V}_{cs}$ as output) and $\hat{\Sigma}^{cs}_{lin}$, we have

$$\left\| \Sigma^{cs}_{lin} - \hat{\Sigma}^{cs}_{lin} \right\|_{H_\infty} \leq \epsilon_{lin}, \quad \epsilon_{lin} = 2\sum_{j=k+1}^{n_c} \sigma_j, \tag{22}$$

where σ_j is the j^{th} Hankel singular value of Σ^{cs}_{lin}.

Finally, the interconnection of the original nonlinear Σ^{cs}_{nl} subsystem and the reduced linear subsystem $\hat{\Sigma}^{cs}_{lin}$ leads to the reduced-order nonlinear system $\hat{\Sigma}^{cs} = (\hat{\Sigma}^{cs}_{lin}, \Sigma^{cs}_{nl})$.

3.2 Properties of original and reduced-order systems

If a number of conditions hold, it can be guaranteed that the described MOR technique preserves stability properties and provides a computable bound on the reduction error in terms of the $\mathcal{L}_2$-induced system norm for the reduced-order nonlinear system $\hat{\Sigma}^{cs}$. These will be stated formally in form of a lemma and theorem in this section.

Two of the above-mentioned conditions are (see Besselink et al. (2013)): 1) the linear subsystem Σ^{cs}_{lin} is asymptotically stable and 2) the small-gain condition

$$\mu^s_{wv}\gamma^s_{vw} < 1, \tag{23}$$

holds, with γ^s_{vw} the (incremental) $\mathcal{L}_2$-gain of Σ^{cs}_{lin} corresponding to $\tilde{W}_{cs}$ as input and $\tilde{V}_{cs}$ as output, and μ^s_{wv} is an upper bound for the incremental $\mathcal{L}_2$-gain of Σ^{cs}_{nl} from $\tilde{V}_{cs}$ to $\tilde{W}_{cs}$. This gain will be computed later.

Lemma 1. If Σ^{cs} satisfies all the aforementioned conditions, then it has a bounded incremental $\mathcal{L}_2$ gain (from input $\tilde{u} = \begin{bmatrix} \tilde{u}_1 & \tilde{u}_2 \end{bmatrix}^T$ to $\tilde{y}$) with bound

$$\gamma_{yu} = \sqrt{2}\max\left(\gamma^s_{yu_1}, \gamma^s_{yu_2}\right). \tag{24}$$

Moreover, the origin is locally asymptotically stable. Here, $M_{sg} := 1 - \mu^s_{wv}\gamma^s_{vw}$ is the small-gain margin, $\gamma^s_{yu_1} = \frac{\gamma_{yv}\gamma^s_{vu_1}}{M_{sg}}$, $\gamma^s_{yu_2} = \frac{\gamma_{yv}\gamma^s_{vw}\mu^s_{wu_2}}{M_{sg}}$, γ_{yv} is the $\mathcal{L}_2$ gain from $\tilde{V}_c$ to $\tilde{y}$, $\gamma^s_{vu_1}$ the incremental $\mathcal{L}_2$ gain from $\tilde{u}_1$ to $\tilde{V}_{cs}$ and $\mu^s_{wu_2}$ is the $\mathcal{L}_2$ gain from $\tilde{u}_2$ to $\tilde{W}_{cs}$.

Theorem 1. If Σ^{cs} satisfies all the aforementioned conditions, the feedback interconnection $\hat{\Sigma}^{cs} = (\hat{\Sigma}^{cs}_{lin}, \Sigma^{cs}_{nl})$ is well-posed and $\hat{\Sigma}^{cs}_{lin}$ is asymptotically stable, the following statements hold:

(1) The reduced-order system $\hat{\Sigma}^{cs}$ has a bounded incremental $\mathcal{L}_2$ gain and the origin is asymptotically stable for $\tilde{u} = 0$ when

$$\mu^s_{wv}(\gamma^s_{vw} + \epsilon_{lin}) < 1, \tag{25}$$

(2) Let (25) hold. Then, the output error $\tilde{y} - \hat{\tilde{y}} = \delta\tilde{y}$ is bounded as $\|\delta\tilde{y}\|_2 \leq \epsilon\|\tilde{u}\|_2$, with $\|.\|_2$ denoting the $\mathcal{L}_2$ signal norm and

$$\epsilon = \sqrt{2}\frac{\gamma^s_{yv}\epsilon_{lin}}{\hat{M}_{sg}} \max(\gamma_1, \gamma_2), \tag{26}$$

where $\hat{M}_{sg} := 1 - \mu^s_{wv}(\gamma^s_{vw} + \epsilon_{lin})$, $\gamma_1 = 1 + \frac{\mu^s_{wv}\gamma^s_{vu_1}}{M_{sg}}$, $\gamma_2 = \frac{\mu^s_{wu_2}}{M_{sg}}$ and γ^s_{yv} is the $\mathcal{L}_2$ gain from $\tilde{V}_{cs}$ to $\tilde{y}$.

Proof. The proof of Lemma 1 and Theorem 1 is based on the results in Besselink et al. (2013).

3.3 Designing the loop transformations

Due to the square root in $f_c(\cdot)$ and the second-degree flow related term, the vector-function $h_c(\cdot,\cdot)$ as in (20) is Lipschitz only locally, implying that the small-gain condition in (23) can hold only locally. This fact, along with the assumption that $z(t) > 0$, provides motivation for restricting our analysis to a particular region Ω_h of the input space of $h_c(\cdot,\cdot)$ (and thus $\tilde{h}_c(\cdot,\cdot)$) defined as

$$\begin{aligned}\Omega_h := \{z, \rho_c, u_2 | z^{min} \leq z \leq z^{max},\\ \rho_c^{min} \leq \rho_c \leq \rho_c^{max}, u_2^{min} \leq u_2 \leq u_2^{max}\},\end{aligned} \tag{27}$$

where the superscripts "max" and "min" denote the maximum and minimum values of a variable.

Now, the matrices H_v, S_w and S_v should be designed such that the small-gain condition is the least conservative, namely M_{sg} is maximized in Ω_h. Here, we take a two-step approach which provides a heuristic for maximizing M_{sg}. In the first step, the matrix H_v is designed such that μ_{vw}, the incremental $\mathcal{L}_2$ norm of $\tilde{h}_c(\cdot,\cdot)$ from $\tilde{V}_c$ to $\tilde{W}_c$, is minimized in Ω_h. One may take (see Besselink (2012))

$$\mu_{vw} = \sup_{\Omega_h} \bar{\sigma}(H(V_c, u_2)),$$

where $\bar{\sigma}(.)$ is the maximum singular value and $H = \partial\bar{h}/\partial V_c - H_v$. As $H(V_c, u_2)$ is diagonal, μ_{vw} can be minimized by minimizing the supremum of each diagonal element over Ω_h. Also, μ^s_{vw} may be computed as

$$\mu^s_{wv} = \sup_{\Omega_h} \bar{\sigma}(S_w H(V_c, u_2) S_v).$$

Next, noting that $h_c(.,.)$ is a multi-input-multi-output mapping, S_v and S_w are designed by solving an optimization problem over Ω_h with M_{sg} as the cost function.

Remark 1. In the presented MOR approach, it has been assumed that the models are completely known, while MPD systems are highly uncertain. But, we project that this model reduction approach is robust and will maintain its performance to a certain extent in the presence of uncertainties that satisfy some norm conditions.

Remark 2. As the small-gain conditions (23) and (25) hold only locally, in order for the Lemma 1 and Theorem 1 to be valid, it is necessary for both the systems Σ^{cs} and $\hat{\Sigma}^{cs}$ to be $\mathcal{L}_\infty$ stable, at least locally, from $\tilde{u}$ to $\tilde{V}_c$ and $\hat{\tilde{V}}_c$, respectively. As both of these systems have asymptotically stable origins, following Corollary 5.3 of Khalil (2014), it can be shown that the systems are locally $\mathcal{L}_\infty$ stable.

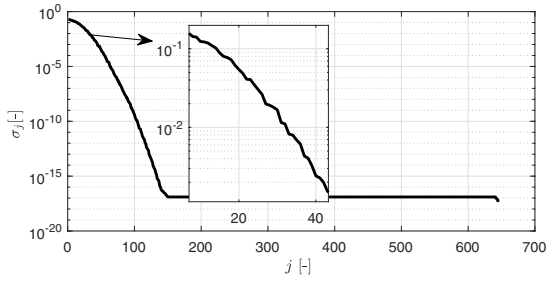

Fig. 3. The singular values σ_i of the linear subsystem Σ^{cs}_{lin}.

4. AN ILLUSTRATIVE CASE STUDY

To evaluate the accuracy of the reduced-order model obtained by the procedure discussed in Section 3, simulations are performed with the parameters listed in Table 1. The nominal inputs are taken as $J^*_{pump} = 54$ kg/s and $z^*_c = 0.3$. We choose the region Ω_h, as in (27), to be bounded by $p_c^{min} = 3$ bar, $p_c^{max} = 32$ bar (can be stated in terms of ρ_c using (2)), $z^{min} = 10$ kg/s, $z^{max} = 60$ kg/s, $z_c^{min} = 0.1$ and $z_c^{max} = 0.32$ (convertible to u_2 using (16)). With this choice, the real part of each eigenvalue of A_c is smaller than -0.1876, implying the asymptotic stability of Σ^{cs}_{lin}, $\mu^s_{wv} = 2.051$ and $\gamma^s_{vw} = 0.413$ and, thus, $\mu^s_{wv}\gamma^s_{vw} = 0.847$ can be achieved, thereby permitting the application of the described nonlinear MOR procedure to our system. It should be noted that μ^s_{wv} can be made significantly smaller by increasing p_c^{min} by a few bars, as $f_c(\rho_c)$ has a high slope for ρ_c close to ρ_0.

The Hankel singular values of the high-order linear subsystem are shown in Fig. 3. Clearly, a relatively fast decay begins around $j = 20$. Here, we choose $k = 41$, for which $\epsilon_{lin} = 0.0194$ and the condition (25) holds with $\hat{M}_{sg} = 0.111$. In Fig. 4, a comparison is performed between the 2×2 transfer function matrices G^s_{vw} of Σ^{cs}_{lin} from $\tilde{W}_{cs}$ to $\tilde{V}_{cs}$ and $\hat{G}^s_{vw}$ of $\hat{\Sigma}^{cs}_{lin}$ from $\hat{\tilde{W}}_{cs}$ to $\hat{\tilde{V}}_{cs}$. Clearly, at low frequencies there is good match between the two linear subsystems, and the resonance frequencies are also well captured by the reduced subsystem.

Remark 3. The normal drilling operations are performed so slowly that the high-frequency modes of the system are seldomly exited. But, there are undesirable scenarios, such as choke plugging and heave motion, that excite these modes and cause transient and periodic pressure fluctuations. Thus, for effective compensation of such fluctuations, it is important that the hydraulics model is able to capture the major resonance frequencies of the system, which indeed approximate the wave propagation phenomenon.

In time domain simulations, the choke opening is decreased from its nominal value z^*_c to $z_c = 0.15$ with a step change

Table 1. The simulation parameters.

Par.	Value	Par.	Value	Par.	Value
l	1817 m	c_l	745 m/s	μ_m	0.04 kg/sm
$\theta(x)$	61.7^o	ρ_0	1800 kg/m^3	C_d	0.8
ϕ^a	0.026 m^2	p_0	1 bar	A_n	7.46×10^{-4} m^2
ϕ^d	0.01 m^2	k_c	0.0032	Δl	40 m
n	160	n_c	645	g	9.81 m/s^2

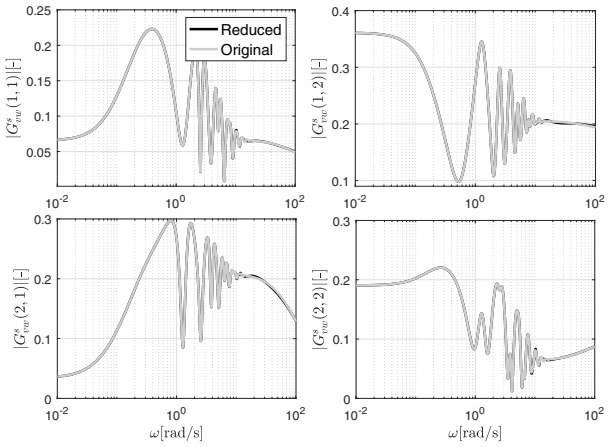

Fig. 4. A comparison between the frequency responses of Σ^{cs}_{lin} and $\hat{\Sigma}^{cs}_{lin}$ from $\tilde{W}_{cs}$ to $\tilde{V}_{cs}$.

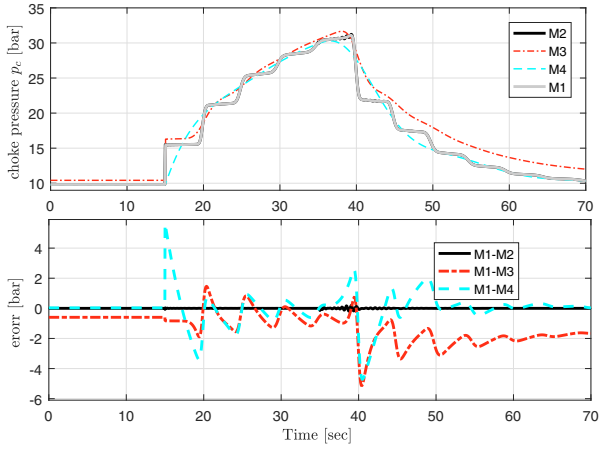

Fig. 5. A time response comparison between M1 the original model Σ^{cs}, M2 the reduced model $\hat{\Sigma}_{cs}$, M3 the model with $n = 9$ and M4 by Kaasa et al. (2012).

at $t = 15$ s, and the pump mass flow rate is reduced to 50% at $t = 35$ s. With these extreme inputs that indeed resemble a choke plugging scenario, a comparison is performed between the original model Σ^{cs} (M1), the reduced nonlinear model $\hat{\Sigma}^{cs}$ (M2) and a model obtained from performing a coarse discretization with $n = 9$ (M3). Note that M3 has the same order as M2. The response of the model presented in Kaasa et al. (2012), shown by M4, is also added as it has a good steady-state accuracy. The results are reported in Fig. 5. This figure shows that the reduced-order model M2 gives a far more accurate approximation compared to the discretized model M3 of the same order, indicating the usefulness of MOR for MPD systems. Moreover, M3 has a better performance in preserving the fast dynamics of the system compared to M4, but it suffers from inaccuracy in steady-state, while M4 has a good steady-state performance.

5. CONCLUSION

A nonlinear model order reduction method has been presented for a managed pressure drilling system. By using a high-resolution discretization scheme and a characteristics-based method for handling the nonlinear boundary conditions a new control-oriented hydraulics model has been derived for the system. The resulting model can be decomposed into a feedback interconnection of a high-order linear and low-order nonlinear subsystem, permitting a model reduction procedure that guarantees preservation of key system (stability) properties and provides a computable reduction error bound in $\mathcal{L}_2$ norm under certain conditions. It has been shown that this conditions hold only locally, implying that the validity of the error bound and preservation of the key properties is only guaranteed in some part of the operating region. Simulations illustrate the effectiveness of the presented model order reduction approach for managed pressure drilling applications.

REFERENCES

Aarsnes, U.J.F., Aamo, O.M., and Pavlov, A. (2012). Quantifying error introduced by finite order discretization of a hydraulic well model. In *2nd Australian Control Conference*, 54–59. Sydney, NSW, Australia.

Besselink, B. (2012). *Model reduction for nonlinear control systems-with stability preservation and error bounds*. Ph.D. thesis, Eindhoven University of Technology, Eindhoven, The Netherlands.

Besselink, B., van de Wouw, N., and Nijmeijer, H. (2013). Model reduction for nonlinear systems with incremental gain or passivity properties. *Automatica*, 49(4), 861–872.

Fernando, K. and Nicholson, H. (1982). Singular perturbational model reduction of balanced systems. *IEEE Transactions on Automatic Control*, 27(2), 466–468.

Fjelde, K.K. and Karlsen, K.H. (2002). High-resolution hybrid primitive-conservative upwind schemes for the drift flux model. *Computers & Fluids*, 31(3), 335 – 367.

Kaasa, G.O., Stamnes, Ø.N., Aamo, O.M., and Imsland, L.S. (2012). Simplified hydraulics model used for intelligent estimation of downhole pressure for a managed-pressure-drilling control system. *SPE Drilling & Completion*, 27(01), 127–138.

Khalil, H.K. (2014). *Nonlinear systems*. Pearson New International Edition. Pearson, Harlow, United Kingdom.

Kurganov, A. and Tadmor, E. (2000). New high-resolution central schemes for nonlinear conservation laws and convection-diffusion equations. *Journal of Computational Physics*, 160(1), 241–282.

Landet, I.S., Mahdianfar, H., Pavlov, A., and Aamo, O.M. (2012). Modeling for MPD operations with experimental validation. In *IADC/SPE Drilling Conference and Exhibition*. Society of Petroleum Engineers, California.

Landet, I.S., Pavlov, A., and Aamo, O.M. (2013). Modeling and control of heave-induced pressure fluctuations in managed pressure drilling. *IEEE Transactions on Control Systems Technology*, 21(4), 1340–1351.

Liu, Y. and Anderson, B.D.O. (1989). Singular perturbation approximation of balanced systems. *International Journal of Control*, 50(4), 1379–1405.

Mahdianfar, H., Aamo, O.M., and Pavlov, A. (2012). Suppression of heave-induced pressure fluctuations in MPD. *IFAC Proceedings Volumes*, 45(8), 239 – 244.

Mahdianfar, H. and Pavlov, A. (2017). Adaptive output regulation for offshore managed pressure drilling. *Int. J. Adapt. Control Signal Process.*, 31(4), 652–673.

Stamnes, Ø.N., Zhou, J., Kaasa, G.O., and Aamo, O.M. (2008). Adaptive observer design for the bottomhole pressure of a managed pressure drilling system. In *2008 47th IEEE Conference on Decision and Control*, 2961–2966. Cancun, Mexico.